Refereed Proceedings

The 12th International Conference on Fluidization - New Horizons in Fluidization Engineering

Engineering Conferences International *Year* 2007

Particle Size Distribution in Gas-Phase Polyethylene Reactors

Omid Ashrafi* Navid Mostoufi†

Rahmat Sotudeh-Gharebagh‡

*University of Tehran

†University of Tehran, mostoufi@ut.ac.ir

‡University of Tehran

PARTICLE SIZE DISTRIBUTION IN GAS-PHASE POLYETHYLENE REACTORS

Omid Ashrafi, Navid Mostoufi* and Rahmat Sotudeh-Gharebagh
Process Design and Simulation Research Center, School of Chemical Engineering,
University of Tehran, P.O. Box 11365/4563, Tehran, Iran
Tel.: (98-21)6696-7781, Fax: (98-21)6646-1024, Email: mostoufi@ut.ac.ir

ABSTRACT

A population balance model is developed to investigate the particle-size distribution developments in a gas-phase fluidized-bed ethylene polymerization reactor. The model considers the combined effects of particle growth and elutriation for size distributed prepolymer feed. In the proposed model, the bed is divided into several sections consisting of bubble and emulsion phases. The population balance differential equations derived for each section were simultaneously solved to determine the density function of the size distribution of the polymer particles in each section. The model is able to predict the axial profiles of particle size distribution. It was also shown that the mean size of the particles is larger at the bottom of the bed and becomes smaller when moving toward top of the reactor.

INTRODUCTION

The gas-phase ethylene polymerization has been long recognized as one of the main processes for producing polyethylene. In this process, small catalyst particles (20-80 μm) as prepolymer are continuously fed into a fluidized bed at a point above the gas distributor and react with the incoming fluidizing gas (monomers) which enters from bottom to form a broad distribution of polymer particles in the size range of 100-2000 μm. Performance of the fluidized bed reactor strongly depends on the hydrodynamic parameters such as minimum fluidization velocity, size of bubbles and gas-solid mass and heat transfer coefficients. These hydrodynamic parameters, in turn, depend on the particle size distribution (PSD). Therefore, a mathematical model capable of predicting the PSD is essential to understand and to optimize the performance of these reactors. However, most of the existing models for predicting the properties of the product and performance of the reactor assume a constant polymer particle diameter for all simulations and do not account for particle size distribution within the bed [1-5].

Despite inherent importance of PSD, limited number of papers has been published on this issue. Zacca et al. [6] developed the population balance model based on the catalyst residence time to model particle size evolution. Choi et al. [7] adopted the population balance approach of Kunii and Levenspiel [8] to investigate the effect of

The 12th International Conference on Fluidization - New Horizons in Fluidization Engineering, Art. 124 [2007]

the feed catalyst size distribution on the product PSD. Khang and Lee [9] applied a population balance approach to investigate the effect of non-ideal mixing behavior of solid particles on the PSD. Hatzantonis et al. [3] formulated and solved generalized steady-state population balance model with counting the effect of particle growth, catalyst deactivation, particle attrition, agglomeration and particle elutriation on the PSD in the gas-phase olefin-polymerization. Harshe et al. [10] presented a comprehensive computational model for predicting PSD.

In the present study, a population balance model is developed based on the hydrodynamic model of Kiashemshaki et al. [12]. In their hydrodynamic model, it was assumed that the fluidized bed reactor for ethylene production contains two phases; each phase is divided into four serial sections. The emulsion phase was considered to be perfectly mixed and the bubble phase was considered to be plug flow in each section. The population balance model differential equations were then developed for each cell and simultaneously solved to determine the PSD of the polyethylene product as well as its profile along the height of the bed.

MODEL DEVELOPMENT

In order to predict the PSD of the reactor, the hydrodynamic and kinetic sub-models should be solved simultaneously together. The results of these sub-models would be used in the population balance model.

Hydrodynamics sub-model

Kiashemshaki et al. [12] showed that a fluidized bed reactor for gas phase polyethylene production could be divided into four sections for each phase. Therefore, in this study, the reactor is considered to be consisted of four continuously stirred tank reactors (CSTRs) for the emulsion phase and four plug flow reactors (PFRs) for the bubble phase. The feed to the reactor enters at top of the first emulsion section (CSTR #4) and leaves the reactor from the bottom of this section (CSTR #1). It was assumed that the bubble phase PSD interacts with the emulsion phase PSD.

Kinetics sub-model

In the present study, the comprehensive mechanism of McAuley et al. [13] was used to describe the copolymerization kinetics of ethylene with 1-butene over Ziegler-Natta catalyst with two different catalyst sites. This mechanism comprises of a series of elementary reactions such as initiation, propagation and chain transfer. Application of the method of moments enables prediction of overall reaction rate for each component [13]:

$$R_n = \sum_{j=1}^{NS} [M_n] Y(0,j) k p_{Tn}(j) \qquad n = 1,2 \tag{1}$$

The cumulative rate of polymer production is calculated from the following:

$$R_{poly} = \sum_{n=1}^{m} (Mw)_n R_n \tag{2}$$

Population Balance Model

A schematic of the fluidized bed reactor of polyethylene is shown in Figure 1. Catalyst particles (as prepolymer) are fed into the bed with a constant flow rate. The amount of polymer in the bed, *W*, is kept constant by controlling the product withdrawal rate at steady state conditions. Inside the bed, the particles grow/diminish in size due to polymerization, agglomeration and attrition. Nevertheless, it should be noticed that it has been assumed that agglomeration and attrition rates could be neglected at the specified operating conditions considered in this work. Particles were assumed spherical with constant density. The PSD in the reactor is specified by the statistical density function, $p_i(D)$. Due to the well-mixed assumption for the particles in each reactor, the density function of the particles in outlet stream is identical to that in each segment, $p_i(D)$.

The steady-state mass balance equation for particles of size *D* is:

$$\left(\frac{F_{in}}{W}\right)p_o(D)-\left(\frac{F_i}{W}+Kr^*(D)\right)p_i(D)-\frac{d}{dr}\left[p_i(D)\psi_p(D)\right]+\frac{d}{dr}\left[p_i(D)\psi_{at}(D)\right] + p_i(D)\frac{3}{D}\left[\psi_p(D)-\psi_{at}(D)\right]+\psi_{ag}(D)=0 \quad (3)$$

In order to derive the equations of the PSD model for each reactor of Figure 1, the terms in Eq. (3) were calculated as follows:

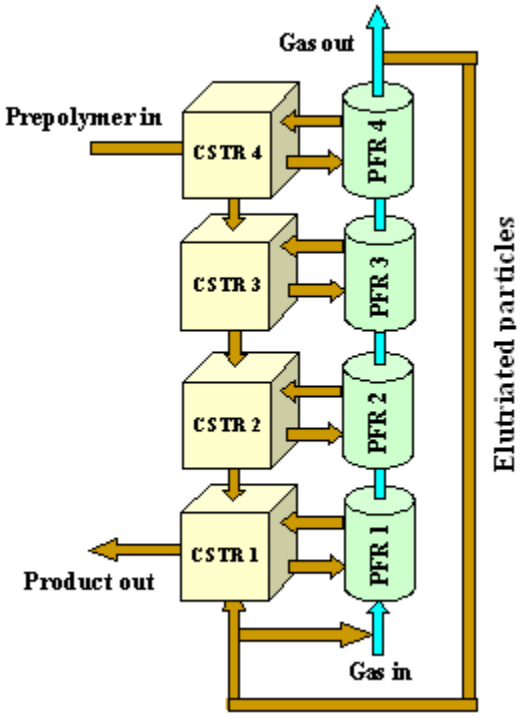

Figure 1. Schematic diagram of the modeling structure

- Since the rate of growth of particles in this model is related only to the polymerization reaction rate, assuming that the radius of the particle in every moment is *r*, the rate of growth of particles could be written as [3]:

$$\psi_p(D)=\frac{dD}{dt}=\frac{D_{cat}^3}{6D^2}\frac{\rho_{cat}}{\rho_p}R_{poly} \quad (4)$$

- The rate of agglomeration was calculated from [3]:

$$\psi_{ag}=k\frac{3D^3}{\pi\rho}\int_{D_c}^{\sqrt[3]{D^3-D_c^3}}\left(d^4+D'^4\right)\times\left(\frac{1}{d^3}+\frac{1}{D'^3}\right)\frac{p_i(D)}{d^5}\frac{p_i(D')}{D'}dD' - k\frac{6p_i(D)}{\pi\rho}\int_{D_c}^{D_{max}}\left(D^4+D'^4\right)\times\left(\frac{1}{D^3}+\frac{1}{D'^3}\right)\frac{p_i(D')}{D'^3}dD' \quad (5)$$

where $d=\sqrt[3]{D^3-D'^3}$, D_c is the minimum particle diameter and D_{max} is the maximum particle diameter.

- The rate of attrition, Ψ_{at}, was considered to be constant [3].
- In Eq. (4), the term corresponding to the elutriation of solids exists only for the top section of the reactor (section #4 in Figure 1). Elutriated solids were

The 12th International Conference on Fluidization - New Horizons in Fluidization Engineering, Art. 124 [2007]

assumed to be totally recycled back to the bottom of the fluidized bed (section #1 in Figure 1) and distributed among both bubble and emulsion phases. The flux of particles carried out of the bed due to elutriation was obtained from:

$$F_e\, p_e(D) = WKr^*(D)\, p_4(D) \tag{6}$$

where the rate of elutriation rate constant is evaluated from [8]:

$$Ki^* = 23.7\rho_g U_0 \exp\left(-\frac{5.4U_t}{U_0}\right) \tag{7}$$

$$Kr^* = Ki^* \frac{A_{bed}}{W_{bed}} \tag{8}$$

The steady state population balance given in Eq. (4) could be applied to each section of Figure 1. Following the approach proposed by Selçuk et al. [14] and using Eqs. (5) to (9), population balance equations of each section would be simplified as follows:

Emulsion Phase

Section 1

$$\frac{dp_{1,e}(D)}{dD} = \frac{1}{\frac{A_1}{D^2} - \psi_{at}} \left\{ \left(\frac{M_{outs,2}\, p_{2,e}(D)}{W} + \frac{M_{outg,1}\, p_{1,b}}{W} + \frac{F_{M,e}\, M_{up}\, p_{4,e}(D)}{W} \right) - \left(\frac{M_{outs,1} + M_{outg,1}}{W} - \frac{5A_1}{D^3} + \frac{3}{D}\psi_{at} \right) p_{1,e}(D) + Kr^* + \psi_{ag} \right\} \tag{9}$$

Section 2

$$\frac{dp_{2,e}(D)}{dD} = \frac{1}{\frac{A_2}{D^2} - \psi_{at}} \left\{ \left(\frac{M_{outs,3}\, p_{3,e}(D)}{W} + \frac{M_{outg,2}\, p_{2,b}}{W} \right) - \left(\frac{M_{outs,2} + M_{outg,2}}{W} - \frac{5A_2}{D^3} + \frac{3}{D}\psi_{at} \right) p_{2,e}(D) + \psi_{ag} \right\} \tag{10}$$

Section 3

$$\frac{dp_{3,e}(D)}{dD} = \frac{1}{\frac{A_3}{D^2} - \psi_{at}} \left\{ \left(\frac{M_{outs,4}\, p_{4,e}(D)}{W} + \frac{M_{outg,3}\, p_{3,b}}{W} \right) - \left(\frac{M_{outs,3} + M_{outg,3}}{W} - \frac{5A_3}{D^3} + \frac{3}{D}\psi_{at} \right) p_{3,e}(D) + \psi_{ag} \right\} \tag{11}$$

Section 4

$$\frac{dp_{4,e}(D)}{dD} = \frac{1}{\frac{A_4}{D^2} - \psi_{at}} \left\{ \left(\frac{M_{in}\, p_0(D)}{W} + \frac{M_{outg,4}\, p_{4,b}}{W} \right) - \left(\frac{M_{outs,4} + M_{outg,4}}{W} - \frac{5A_4}{D^3} + \frac{3}{D}\psi_{at} \right) p_{4,e}(D) + \psi_{ag} \right\} \tag{12}$$

where $A_i = \frac{D_{cat}^3}{3}\frac{\rho_{cat}}{\rho_p} R_{polys}^i$ and $F_{M,e} = \frac{(1-\delta)(1-\varepsilon_e)}{(1-\delta)(1-\varepsilon_e) + \delta(1-\varepsilon_b)}$

Bubble Phase

Section 1

$$\frac{dp_{1,b}(D)}{dD} = \frac{1}{\frac{B_1}{D^2} - \psi_{at}} \left\{ \left(\frac{F_{M,b}\, M_{up}\, p_{4,b}(D)}{W} + \frac{M_{outg,1}\, p_{1,e}}{W} \right) - \left(\frac{M_{upg,1} + M_{outg,1}}{W} - \frac{5B_1}{D^3} + \frac{3}{D}\psi_{at} \right) p_{1,b}(D) + Kr^*\, p_{4,b}(D) + \psi_{ag} \right\} \quad (13)$$

Section 2

$$\frac{dp_{2,b}(D)}{dD} = \frac{1}{\frac{B_2}{D^2} - \psi_{at}} \left\{ \left(\frac{M_{upg,1}\, p_{1,b}(D)}{W} + \frac{M_{outg,2}\, p_{2,e}}{W} \right) - \left(\frac{M_{upg,2} + M_{outg,2}}{W} - \frac{5B_2}{D^3} + \frac{3}{D}\psi_{at} \right) p_{2,b}(D) + \psi_{ag} \right\} \quad (14)$$

Section 3

$$\frac{dp_{3,b}(D)}{dD} = \frac{1}{\frac{B_3}{D^2} - \psi_{at}} \left\{ \left(\frac{M_{upg,2}\, p_{2,b}(D)}{W} + \frac{M_{outg,3}\, p_{3,e}}{W} \right) - \left(\frac{M_{upg,3} + M_{outg,3}}{W} - \frac{5B_3}{D^3} + \frac{3}{D}\psi_{at} \right) p_{3,b}(D) + \psi_{ag} \right\} \quad (15)$$

Section 4

$$\frac{dp_{4,b}(D)}{dD} = \frac{1}{\frac{B_4}{D^2} - \psi_{at}} \left\{ \left(\frac{M_{upg,3}\, p_{3,b}(D)}{W} + \frac{M_{outg,4}\, p_{4,e}}{W} \right) - \left(\frac{M_{up} + M_{outg,4}}{W} - \frac{5B_4}{D^3} + \frac{3}{D}\psi_{at} - Kr^* \right) p_{4,b}(D) + \psi_{ag} \right\} \quad (16)$$

where $B_i = \frac{D_{cat}^3}{3} \frac{\rho_{cat}}{\rho_p} R_{polyg}^i$ and $F_{M,b} = \frac{\delta(1-\varepsilon_b)}{(1-\delta)(1-\varepsilon_e) + \delta(1-\varepsilon_b)}$

By simultaneous solving of ordinary differential equations (9) through (16), the PSD density functions of all sections could be obtained for both bubble and emulsion phases. The PSD of the polymer in each section of the reactor is given by the following expression:

$$p_i(D) = F_{M,e}\, p_{i,e}(D) + F_{M,b}\, p_{i,b}(D) \quad (17)$$

RESULTS AND DISCUSSION

The model was solved for a sample linear low density polyethylene (LLDPE) produced at an industrial plant in Iran. The parameters and operating conditions used in the simulation are listed in Table 1. A comparison between the actual PSD of the product and the PSD calculated by the model is shown in Figure 2 in terms of cumulative PSD. The cumulative PSD of the feed is also shown in the same figure. It could be seen in this figure that the calculated PSD is in good agreement with the

The 12th International Conference on Fluidization - New Horizons in Fluidization Engineering, Art. 124 [2007]

actual PSD. Even though the calculated distribution is somewhat sharper than the actual, the mean size of the product is properly predicted by the model.

Table 1. Operating conditions used in the simulation

Parameter	Value	Unit
ρ_g	21	kg/m^3
ρ_{cat}	2840	kg/m^3
ρ_p	920	kg/m^3
Ψ_{at}	10^{-6}	kg/s
k	10^{-7}	kg/(m.s)
U_0	0.25	m/s
F_{in}	0.5	kg/s

In fact, Figure 2 reveals that although the model correctly predicts the average growth of the polymer particles, it under predicts the growth of the finer particles while over predicts the growth of courser particles. This shortcoming of the model could be contributed to the fact that the rate of polymerization, R_{poly}, was assumed to be independent of the size of the particles. However, the rate of polymerization in large particles is less than the rate in small particles. This is the reason for the difference seen in Figure 2 between the experimental and simulated data values.

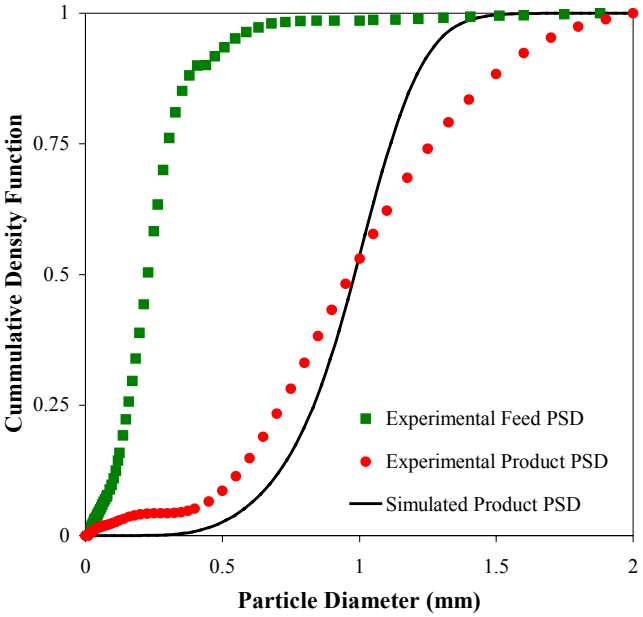

Figure 2. Comparison between actual and simulated PSDs

Figure 3 illustrates the averaged PSD in each section of the reactor. Each distribution in this figure has been obtained by means of averaging the PSDs of bubble and emulsion in each section by weight of polymer according to Eq. (17). Figure 3 reveals that the mean size of the particles in the reactor increases when moving downward due to the fact that emulsion phase contains more solids than bubble phase. In other words, larger particles tend to exist at the bottom of the reactor while there are more small particles at the top. This phenomenon, although very well known, had not been quantified before. It could be seen in Figures 3 that the PSD of the polymer becomes sharper when moving toward the bottom of the reactor. The reason for such a trend is that in spite of the fact that the particles grow larger when moving down the reactor, the rate of production becomes higher for fine particles. The finer particles (corresponded to the left tail of the PSD curve) grow faster than larger particles (corresponded to the right tail of the PSD curve), thus, the PSD curve becomes less wide as the particles move down the reactor and their mean size becomes larger.

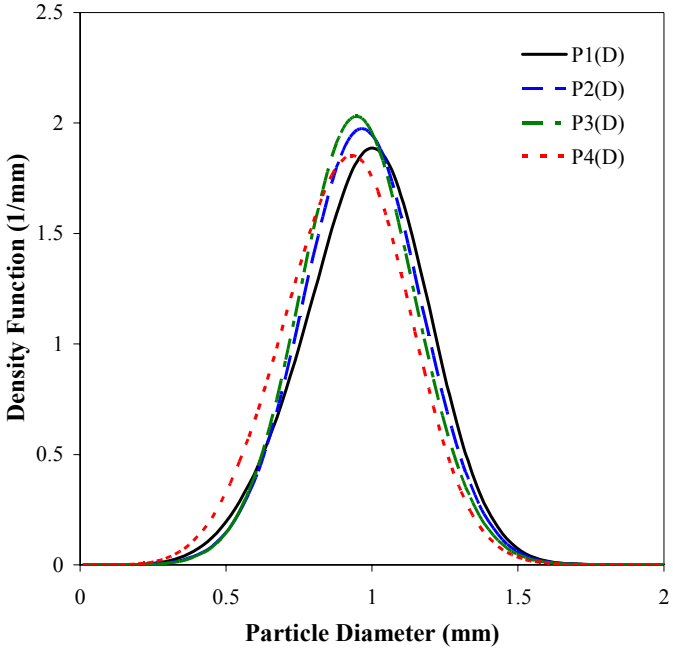

Figure 3. Predicted PSD of polymer along the height of the reactor at U_0=0.25

An important outcome of the model developed in this work is that it can determine the axial profile of the PSD in the reactor. In fact, since the sections of this model are located one on top of another, the mean particle size in each segment could be attributed to the size of the particles at the corresponding height of the bed. Figure 4 illustrates the axial profiles of the mean particle size in the reactor. As could be seen in this figure, finer particles are situated at the top of the reactor while larger particles are found at the bottom. It is worth noting that based on the model presented in this work, development of such an axial profile occurs only as a result of growth of the particles due to polymerization reactions while they move down the reactor in emulsion phase and move upward in bubble phase.

The 12th International Conference on Fluidization - New Horizons in Fluidization Engineering, Art. 124 [2007]

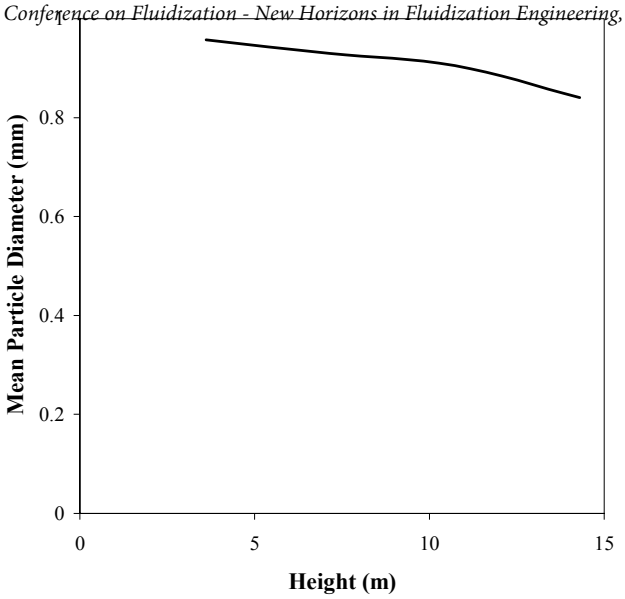

Figure 4. Axial profile of mean particle size of polymer in the reactor

CONCLUSIONS

A mathematical model is developed for predicting the PSD of polymer particles in the gas phase polyethylene reactor. This model is able to provide the axial profile of the particle size. A generalized framework based the model of Kiashemshaki et al. [12] and the two-site kinetic scheme of McAuley et al. [13] was developed for calculating the PSD. It was shown that smaller particles exist at the top of the reactor while larger particles tend to present at the bottom of the reactor. A new feature in the proposed model is that it is able to predict the axial profile of the mean particle diameter in the reactor.

NOTATION

A_i	[kg.m^3/s]	coefficient used in emulsion equations
A_{bed}	[m^2]	bed area
B_i	[kg.m^3/s]	coefficient used in bubble equations
D	[m]	diameter of particle
D_{cat}	[m]	diameter of prepolymer
F_e	[kg/s]	elutriated mass flow of polymer from the reactor
F_i	[kg/s]	mass flow of polymer leaving CSTR *i*
$F_{M,\,e}$		mass fraction of particles in emulsion
$F_{M,\,b}$		mass fraction of particles in bubbles
kp_{Ti}	[m^3/kmol.s]	propagation rate constant
Kr^*	[1/s]	rate of elutriation
Ki^*	[kg/m^2.s]	elutriation rate constant
k	[kg/m.s]	agglomeration constant
M_n	[kmol/m^3]	concentration of monomer type *n*
M_{up}	[kg/s]	mass flow of elutriated particles
$M_{outs}i$	[kg/s]	product mass flow of polymer from emulsion phase for CSTR *i*
$M_{upg}i$	[kg/s]	product mass flow of polymer from bubble phase for PFR *i*

$M_{outg}i$	[kg/s]	mass flow of particles between tow phases
$(Mw)_k$	[kg/kmol]	molecular weight of monomer k
NS		number of types of active sites on the catalyst
$p_e(D)$	[1/m]	density function in elutriation stream
$p_o(D)$	[1/m]	density function in feed
$p_{i,e}(D)$	[1/m]	density function of outlet stream from CSTR i
$p_{i,b}(D)$	[1/m]	density function of outlet stream from PFR i
R_n	[kmol/s]	rate of consumption of component n
R^i_{ploys}	[kg/s]	rate of polymerization in CSTR i
R^i_{ploys}	[kg/s]	rate of polymerization in PFR i
t	[sec]	time
U_0	[m/s]	superficial gas velocity
U_t	[m/s]	terminal velocity of particles
W	[kg]	weight of each segment
$Y(0,j)$	[kmol]	zero moment of living polymer chain

Greek letters

ρ_g	[kg/m^3]	gas density,
ρ_p	[kg/m^3]	polymer density
ρ_{cat}	[kg/m^3]	catalyst density
Ψ_p	[m/s]	rate of particle growth
Ψ_{at}	[m/s]	rate of particle corrosion due to attrition
Ψ_{ag}	[1/m.s]	rate of particle growth due to agglomeration
ε_e		emulsion void fraction
ε_b		bubble void fraction
δ		bubble fraction

Subscripts

i	segments no.
j	active site type no.
m	number of types of monomers
n	monomer no.

REFERENCES

[1] K.Y. Choi, W.H. Ray, *Chem. Eng. Sci.*, *40*, 2261, (1985).
[2] K.B. McAuley, J.P. Talbot, T.J. Harris, *Chem. Eng. Sci.*, *49*, 2035, (1994).
[3] H. Hatzantonis, A. Goulas, C. Kiparissides, *Chem. Eng. Sci.*, *53*, 3251, (1998).
[4] F.A.N. Fernandes, L.M.F. Lona, *Chem. Eng. Sci.*, *56*, 963, (2001).
[5] M. Alizadeh, N. Mostoufi, S. Pourmahdian, R. Sotudeh-Garebagh, *Chem. Eng. J.*, *97*, 27, (2004).
[6] J.J. Zacca, J.A. Debling, W.H. Ray, *Chem. Eng. Sci.*, *51*, 4859, (1996)
[7] K.Y. Choi, X. Zhao S. Tang, *J. App. Polym. Sci.*, *53*, 1589, (1994).
[8] D. Kunii, O. Levenspiel, *Fluidization Engineering*, 2nd ed., Butterworth-Heinmen, Boston, MA, (1991).
[9] D.Y. Khang, H.H. Lee, *Chem. Eng. Sci.*, *52*, 421, (1997).
[10] Y.M. Harshe, R.P. Utikar, V.V. Ranadeh, *Chem. Eng. Sci.*, *59*, 5145, (2004).
[11] R. Jafari, R. Sotudeh-Gharebagh N. Mostoufi, *Chem. Eng. Technol.*, *27*, 123, (2004).
[12] A. Kiashemshaki, N. Mostoufi, R. Sotudeh-Gharebagh, *Chem. Eng. Sci.*, *61*, 3997, (2006).

[13] K.B. McAuley, J.F. MacGregor, A.E. Hamielec, *AIChE J.*, 36, 837, (1990).
[14] N. Selçuk, O. Oymak, and E. Değirmenci, *Powder Technol.*, 87,269, (1996).